HEFAT2008
6th International Conference on Heat Transfer, Fluid Mechanics and Thermodynamics
30 June to 2 July 2008
Pretoria, South Africa
Paper number: LP1

Optical diagnostics development and coupling dedicated to heat, mass and aerosol transfers in a spray for severe accident safety analysis in nuclear power plant

Pascal LEMAITRE, Emmanuel PORCHERON, Amandine NUBOER

Institut de Radioprotection et de Sûreté Nucléaire (IRSN)

BP 68, 91192 Gif-sur-Yvette cedex, France

Phone : +33 1 69085072, FAX : +33 1 69089736

Pascal.lemaitre@irsn.fr

Keywords
Thermal hydraulic, optical diagnostics, TOSQAN, Spray, Heat and mass transfers, Aerosol collection

ABSTRACT In order to study the interactions between a spray and an atmosphere representative of a severe accident in a Pressurized Water Reactor, in terms of pressure, temperature and composition (steam and aerosol), the French Institute for Radiological Protection and Nuclear Safety (IRSN) developed the TOSQAN facility. This paper presents the development and qualification of the global rainbow refractometry and Interferometric Laser Imaging for Droplets Sizing (ILIDS) that are respectively dedicated to measure the spray droplets temperature and size. In addition we present an extension of these two techniques in order to determine the aerosol concentration inside the droplet and the aerosol removal rate.

NOMENCLATURE

Latin

d : Diameter	[m]
f : Angular frequency	[deg^{-1}]
T : Temperature	[°C]
P : Pressure	[Pa]
Q : Mass flow rate	[$kg.s^{-1}$]
f(d) : Probability density function	[-]
n_e : Index of refraction outside the droplet	[-]
n_i : Index of refraction inside the droplet	[-]
m : $m = \frac{n_i}{n_e}$	[-]
k : Imaginary part of the optical index	[-]
p : Scattering mode	[-]

Greek

θ : Scattering angle	[deg]
λ : Wavelength	[m]

INTRODUCTION

During the course of a hypothetical severe accident in a nuclear Pressurized Water Reactor (PWR), hydrogen, radioactive aerosols and steam can be produced and distributed into the reactor containment according to convection flows, water steam wall condensation and interaction with the spray droplets.
In order to assess the risk of a detonation generated by a high local hydrogen concentration, hydrogen distribution in the containment has to be known.

The TOSQAN experimental program has been launched to simulate experimentally typical accidental thermal hydraulic flow conditions of the reactor containment and to study different phenomena such as water steam condensation on droplets in presence of non-condensable gases and aerosol removal by droplets.
This large experimental facility (7 m^3) is suitable for optical diagnostics: therefore the PIV, LDV, Spontaneous Raman Scattering and global rainbow refractometry are already implemented on it [6, 7].
In order to measure droplets size, different non-intrusive techniques were envisaged like Phase Doppler Anemometry (PDA) [1] and Interferometric Laser Imaging for Droplets Sizing (ILIDS) [2]. Because of TOSQAN geometrical conditions, we selected the last one.
Our work on the interferometric laser imaging technique is presented in this paper, that is divided into four parts. The first one explains the principle of the ILIDS technique, and the optical phenomenon on which it is based on. This part is illustrated with Lorenz-Mie Theory (LMT) simulations.
In the second part, we present the qualification of the ILIDS technique using comparisons with PDA and backscattering measurements performed respectively on a full cone spray and on a drop-by-drop jet. In the third part, we present the implementation of the technique on the

TOSQAN experiment and the associated droplets measurements.

Then the same approach is followed on the global rainbow technique used for measuring droplets temperature.

On addition to that, in PWR, spray droplets are used for airborne aerosols washout. If the aerosol particles are soluble, the washout induces variations in both the imaginary and real parts of the droplets optical index. These variations of the index of refraction induce a decrease of the fringes contrast for the ILIDS technique and a translation of the geometrical rainbow angle for the rainbow technique.
Thus, we present in this last part a reference experiment that highlights the feasibility of the measurement of the imaginary part of the droplets index of refraction, using the ILIDS technique.

1 OPTICAL PRINCIPLE AND GENERAL BACKGROUND

1.1 General principle

In this first part of the paper, we recall the principle of Interferometric Laser Imaging for Droplets Sizing ILIDS, an optical diagnostic dedicated to measuring droplets size. This out-of-focus imaging diagnostic has first been introduced by Glover [2]. It allows determining droplets size in a poly-dispersed spray. A model based on geometrical optics is generally accurate enough to describe this technique which is based on the analysis of the interferences generated by externally reflected (p = 0) and refracted rays p = 1 (Figure 1).

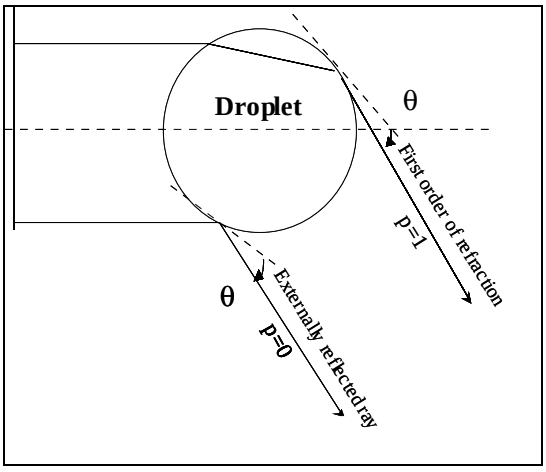

Figure 1. Out-of-focus imaging principle

In the focal plane these two scattering modes generate bright spots called glare points (Figure 2).
The size of the particle can be determined by measuring the distance between these two points [9].

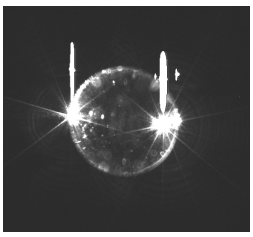

Figure 2. Glare points observation (θ = 67°, incident parallel polarization)

The distance between these glare points is a few tens of microns, thus it requires a very high resolution to determine precisely the droplets size. Another way to determine the droplets size is to defocus the optical set-up. Thus, fringes appear due to interferences between reflected and refracted rays (p = 0 and p = 1, Figure 3).

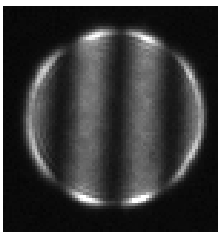

Figure 3. Fringes observation in the out-of-focus plan

The relationship linking the angular frequency of the fringes (f) and the droplet size (d) can be determined using geometrical optics, by calculating the optical path difference between reflected and refracted rays.

$$d = \frac{2\lambda f}{n_e}\left(\cos\left(\frac{\theta}{2}\right) + \frac{m\sin\left(\frac{\theta}{2}\right)}{\sqrt{\left(m^2 - 2m\cos\left(\frac{\theta}{2}\right) + 1\right)}}\right) \quad (1)$$

In this equation, m is the ratio between the internal and external index of refraction, n_e the index of refraction of the medium outside the droplet, λ is the wavelength of the incident wave and θ the scattering angle.

In order to validate the use of geometrical optics, we make comparison with the Lorenz Mie Theory (LMT), which consists in resolving analytically the Maxwell equations inside and outside the droplet [5] (Figure 4 and Figure 5).

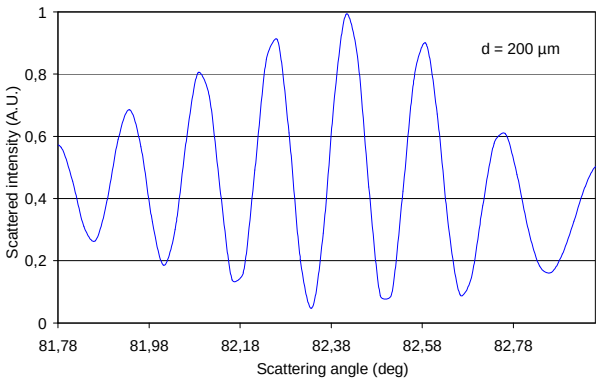

Figure 4. Fringes computation using Lorenz Mie Theory

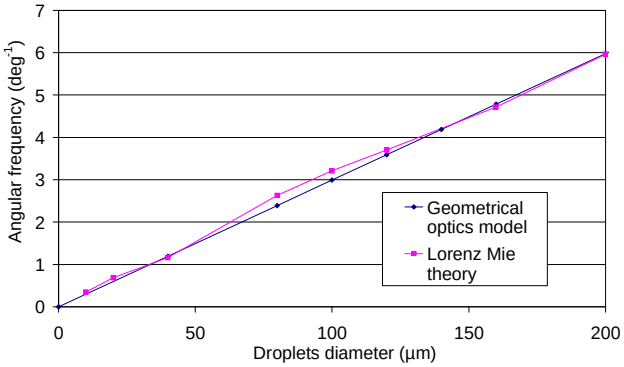

Figure 5. Validity of the geometrical optics model

This comparison is achieved for an incident wave $(\lambda = 532\,nm)$ polarized parallelly to the scattering plane, and for a water droplet in air (m = 1.33, n_e = 1).
The frequency of the fringes is computed for a scattered angle near θ = 80°.
We thus validate the use of geometrical optics near the scattering angle of 80°. In order to have the best contrast of the fringes, we compute the intensity of each scattering mode (by computing the Fresnel coefficients) and look for the angle at which we obtain the same intensity for reflected and refracted rays. On Figure 6, p corresponds to the scattering mode.
Thus, p = 0 corresponds to externally reflected rays, p = 1 to refracted rays, p = 2 to internally reflected rays and so on. We observe on these simulations that for an incident wave perpendicularly (respectively parallelly) polarized, the intensities of reflected and refracted rays are equal for a scattering angle of 67° (respectively 80°). On addition to that, we observe that whatever the polarization of the incident wave, the intensity of refracted rays falls down to zero at about 82°. However, the LMT still predicts fringes, for an incident wave parallelly polarized (Figure 7). Thus, near θ = 90°, the geometrical optics model is not available anymore. A special calibration curve needs to be computed using LMT. This calibration curve is presented on Figure 8.

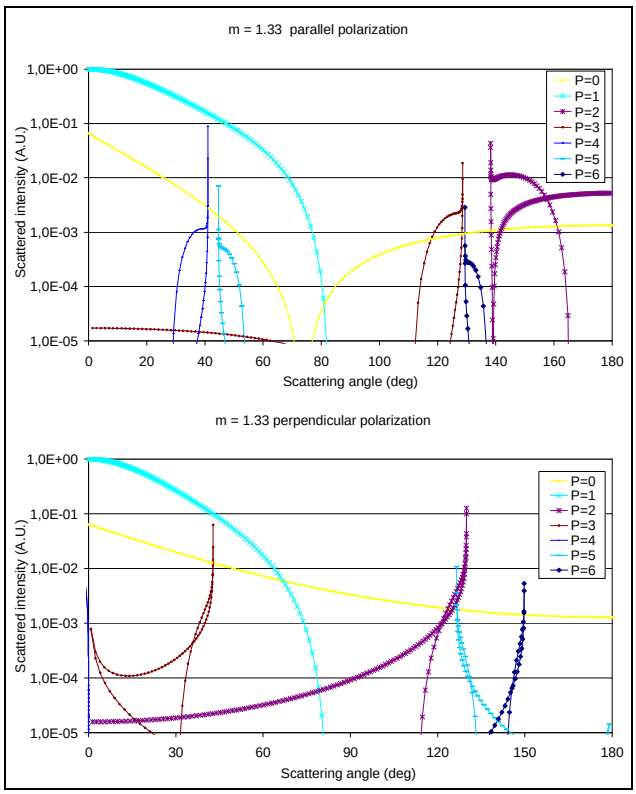

Figure 6. Evaluation of the scattering diagram of droplets

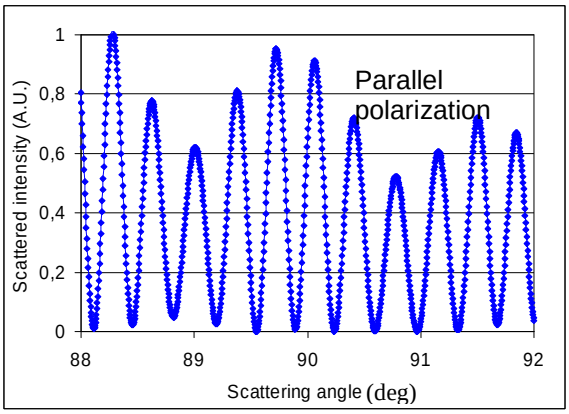

Figure 7. Fringe pattern computed using LMT

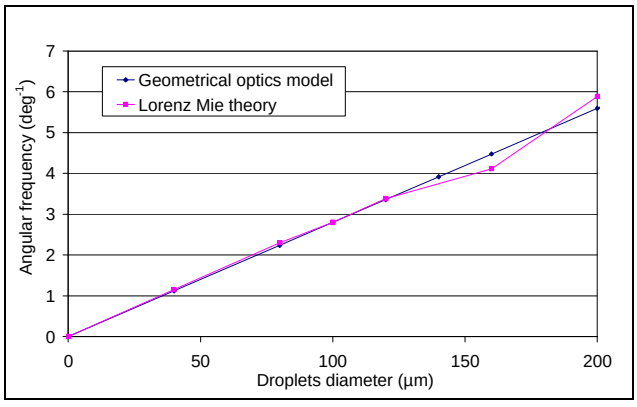

Figure 8. Calibration curve at 90°

It is of interest to notice that, even if the geometrical optics model is not suitable to correctly predict the intensity of the scattering modes near 90° (Figure 6), the LMT simulation presented on Figure 8 shows that equation 1 deduced from the geometrical optics model is still acceptable to compute the relationship between the droplets diameter and the angular frequency of the fringes. This observation is very important because, in our application of out-of-focus imaging, the measurement will be achieved at a scattering angle of 90°, due to the limitations in the optical accesses of the TOSQAN facility.

1.2 Influence of the droplets temperature

For our measurements inside the TOSQAN facility, heat and mass transfers occur between the droplets and the gas. As a consequence, droplets temperature is not precisely known during the out-of-focus measurement.
In this part, we focus on the sensitivity of the relationship between the angular frequency of the fringes and the droplets size, for different droplets temperature, thus for different index of refraction (Figure 9).
Thus, we compute the theoretical relationship between the angular frequency and the droplets size near an off axis angle of 80° but for different droplets temperature using LMT. Figure 9 presents the relationship linking water index of refraction and its temperature [10].

Table 1. Relationship linking water index of refraction and temperature (λ = 532 nm)

T (°C)	m
50	1.3309
90	1.3223
100	1.3196

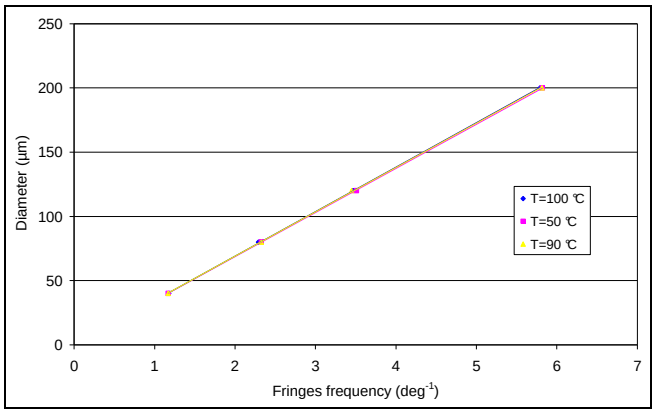

Figure 9. Influence of the droplet's temperature on the relationship between the frequency of the fringes and the droplets size

Thus, we observe on this simulation that the index of refraction variations induced by the droplets heating does not disturb the relationship between the droplets diameter and the frequency of the fringes. Consequently, this technique is able to give a precise droplet size measurement, without any previous knowledge of its temperature.

2 EXPERIMENTAL QUALIFICATION OF THE OUT-OF-FOCUS TECHNIQUE

2.1.1 Validation on optical table

In order to validate the droplet size deduced from the ILIDS technique, backscattering and out-of-focus imaging measurements are performed simultaneously on a drop-by-drop jet. The scheme of this experiment is presented on Figure 11.

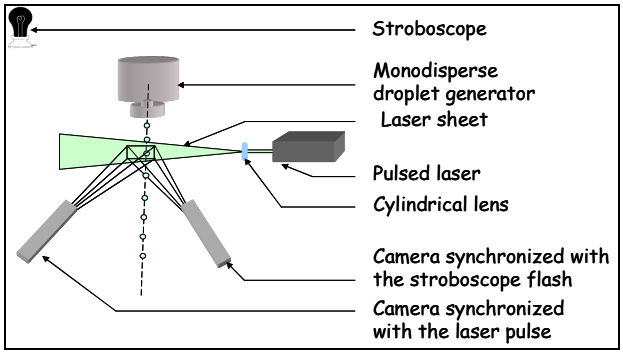

Figure 10. Scheme of the experiment

For this measurement the laser is polarised perpendicularly to the scattering plan. As a consequence, the collecting camera is placed at a 66° off axis angle, in order to have the better fringe contrast (Figure 6). Concerning the backscattering imaging set-up, it is composed of a stroboscope which flash is synchronized with the camera's opening. This camera is a folding one in order to increase the magnification factor of the collecting optics. The magnification factor of this collecting optics is 1.4 µm per pixel.

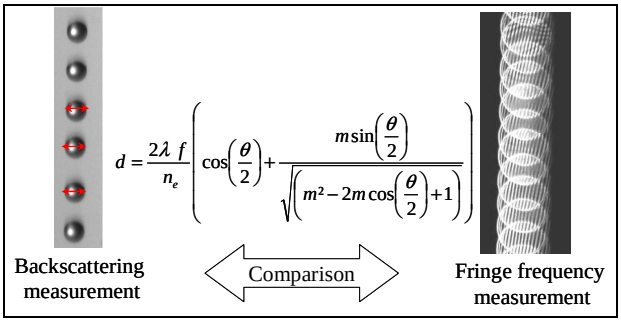

Figure 11. Example of measurements

The comparison between these two measurements is presented on Figure 12. We observe a good agreement between these simultaneous measurements because the slope of the interpolation line is very close from one. The small difference between these measurements might be explained by the fact that these two measurements are not achieved in exactly the same plane that can cause little differences in the droplet diameter measurement if the droplets are not perfectly spherical.

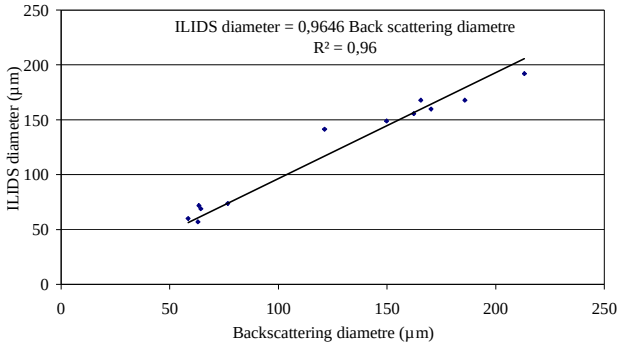

Figure 12. Comparison between ILIDS and backscattering measurements

2.1.2 Validation on a full cone spray

A second step validation is achieved on a full cone spray with PDA measurements. These measurements are achieved using a commercial DANTEC PDA and compared with the out-of-focus imaging technique. The PDA measurements are achieved at an off axis angle (θ) equal to 72°, and with an incident light parallely polarized. This angle corresponds to the Brewster angle for water. At that angle, the intensity of reflected light falls to zero (Figure 6). This comparison is performed on the spray produced by a TG_3.5 nozzle operating with a water mass flow rate of 30 $g.s^{-1}$, at a distance of 1 m from the orifice of the nozzle. These measurements are not achieved simultaneously, but with exactly the same temperature and pressure conditions for the injected water and for the surrounding gas for the PDA and ILIDS measurements.
As these measurements are achieved with the same conditions for the surrounding gas (pressure, temperature and saturation ratio) and for injection conditions (same nozzle, same water mass flow rate and same temperature), we make sure that the atomization process is exactly the same and on addition to that, we ensure that we have exactly the same droplets vaporization rate. As a consequence, the measurement should be exactly the same. The droplets size distribution measured with the ILIDS technique is presented on Figure 13.

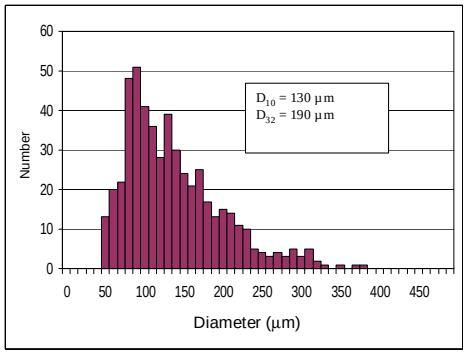

Figure 13. Measurement achieved with the ILIDS technique

The histogram of diameter is well fitted using a log-normal distribution. The arithmetic mean diameter D_{10} and the Sauter mean diameter D_{32} are respectively equal to 130 µm and 190 µm. The arithmetic mean diameter and the Sauter mean diameter are respectively computed using equation 2.

$$D_{ij} = \frac{\int_0^\infty d^i \cdot f(d)dd}{\int_0^\infty d^j f(d)dd} \quad (2)$$

The histogram measured with the PDA technique can be as well fitted using a log-normal distribution, but the arithmetic mean diameter of the droplets is now equal to 115 µm, which represents a difference of 12 %. This difference might seem important but it is mainly explained by the difference of measurement dynamic of these two techniques, which is more important for the ILIDS technique.
To confirm this hypothesis, we impose artificially to ILIDS measurements the same measurement range than for PDA ones, the new arithmetic mean diameter computed is 116 µm (115 µm with the PDA).
This allows us to validate our previous hypothesis on the origin of the difference between the measurements using these two techniques, and finally to validate the ILIDS measurement.

3 MEASUREMENT INSIDE THE TOSQAN EXPERIMENT

3.1 Experimental set-up

As mentioned in the introduction, the TOSQAN experimental program has been launched to simulate typical accidental thermal hydraulic flow conditions of the reactor containment and to study different phenomena such as water steam condensation on droplets in presence of non-condensable gases.
This large experimental facility presented on Figure 14 is 4 m height, with an internal diameter of 1.5 m. Droplets can be injected in the upper part of the experiment using a single nozzle.
On addition to that, the experiment is equipped with 14 viewing porthole windows, placed at 90° the one from the other on four levels (Figure 14).

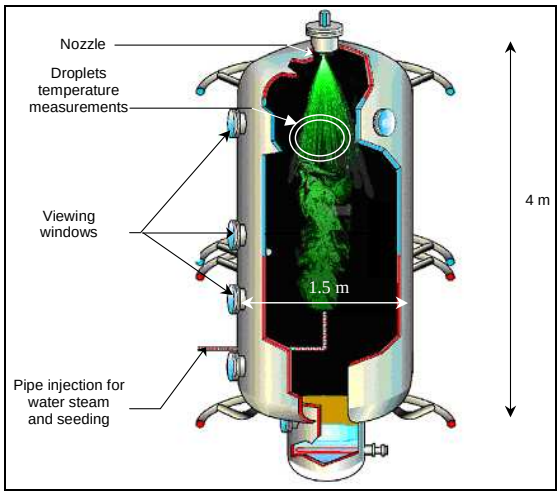

Figure 14. Overview of the TOSQAN Facility

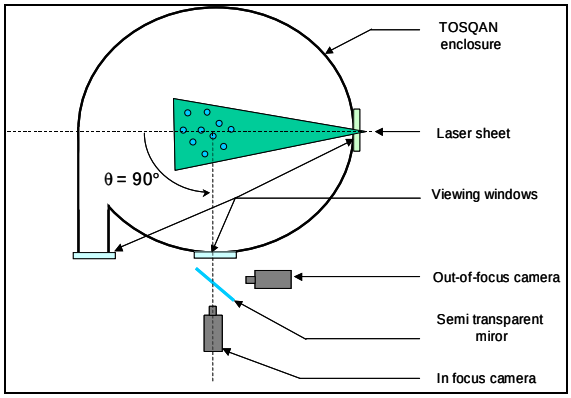

Figure 15. Scheme of the optical set-up implemented on the TOSQAN experiment

The optical set-up adopted to achieve droplets size measurements inside the TOSQAN experiment is presented on Figure 15.

The coherent light necessary for this technique issues from a pulsed Nd : Yag laser (λ=532 nm). The laser beam is then extended using a cylindrical lens in order to create a laser sheet. The width of this laser sheet is about 1 mm.
As the TOSQAN experiment is equipped with viewing windows with 90° angle the one from the other, we work with an incident laser beam parallely polarized in order to have the best fringe contrast (part 1.1).
The cameras used are High-Sense CCD cameras with 1024×1280 pixel².

Inside the TOSQAN experiment, the droplets density is important, thus this creates overlapping between the fringes pattern from different droplets.
That overlapping (Figure 16) makes the measurement of the fringe frequency difficult to perform.

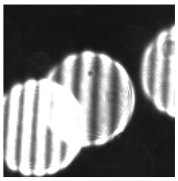

Figure 16. Fringe pattern overlapping

Thus, to simplify the processing of the measurement, a second camera is used (Figure 15).

3.2 Image processing

The second camera is focused in the laser sheet plan and thus observes the glare points of the droplets. These two cameras are placed in order to observe the same field. The focused camera detects the glare points using the same algorithm as for the PIV technique. Thus, knowing the degree of defocusing (γ), the focal length of the collecting system (f) and the dimension of the optical aperture (L), we compute the dimension (T) of each interferometric images in the out-of-focus image $T = L\frac{\gamma}{f}$.

As a consequence, we can determine the non overlapping zones using the position of the glare points on the focused image and the size of the defocused image T.
Knowing the non overlapping areas, on the defocused image we achieve a 2 Dimensional Fast Fourier Transform (2D FFT) to determine the fringes frequency. Finally, using the calibration curve determined with the help of the LMT, we deduce the droplets diameter.

3.3 Experimental results

This set-up has been applied to the TOSQAN experiment during the 101 spray test [8]. This one is included in a benchmark [3] dedicated to validate the capacity of different CFD codes to simulate the transfers between droplets and gas for thermal hydraulic conditions representative of a hypothetical nuclear accident in a PWR.

The thermal hydraulic conditions during the measurement are presented in Table 2.

Table 2. Thermal hydraulic conditions during the droplets size measurement

T_{gas} (K)	P_{vap} (bar)	P_{air} (bar)	Q_{spray} ($g.s^{-1}$)
378.5	1.15	1	30

Figure 17 presents an example of defocused image obtained with this experimental set-up.
The analysis of about 20 images allows us to determine the droplets size distribution, presented on Figure 18.

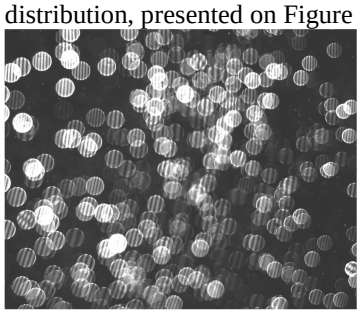

Figure 17. Example of out-of-focus image

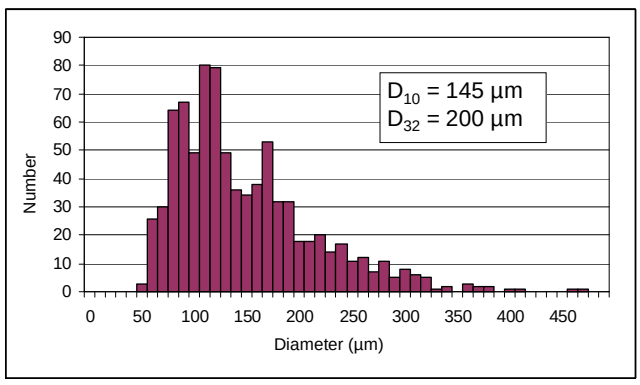

Figure 18. Droplets size distribution measured during the 101 spray test

These measurements are useful in order to characterize heat and mass transfer processes between the droplets and the gas [8].

4 EXTENSION OF THE TECHNIQUE

During the course of a hypothetical accident, with fusion of the core, radioactive aerosol might be produced and distributed into the containment vessel. The spray release is one of the mitigation technique used to collect these harmful particles, and thus to washout them from the containment vessel [4].

With the aim of characterizing the phenomena involved in the aerosol collection by a droplet (inertial impaction, interception, phoretic effects) [4], it would be useful to measure the mass of aerosols collected by the droplets.

If we put emphasis on in soluble aerosol particles, their collection by the droplets induces a variation of the imaginary part of their index of refraction. A solution to quantify the number of aerosol particles collected by the droplets is thus to measure their optical index imaginary part.

As mentioned in part 1, the contrast of the fringes depends on the ratio of intensity of the scattering mode (p = 0 and p=1). It is maximum when these two modes are equal. Moreover, when the droplets are optically absorbents, the intensity of the mode p = 1 decreases and, as a consequence, for the same optical configuration, there is a modification on the fringe contrast.

Thus, it would be of interest to find an optical configuration for which a biunivocal relationship exists between the contrast of the fringes and the imaginary part on the optical index (k).

Different simulations were achieved using the LMT, for different scattering angles and different polarizations of the incident wave.

The influence of the imaginary part of the optical index is highlighted in Figure 19. This simulation is achieved with an incident wave perpendicularly polarized.

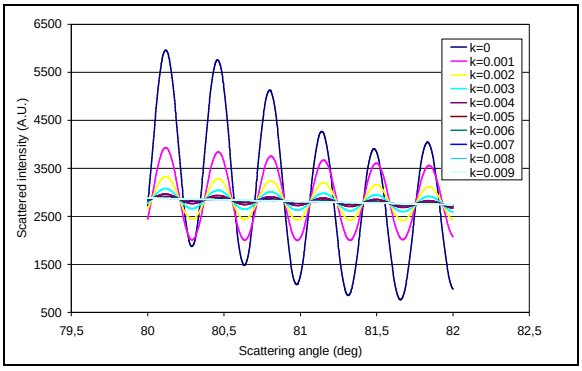

Figure 19. Influence of the imaginary part of the optical index on the contrast of the fringes

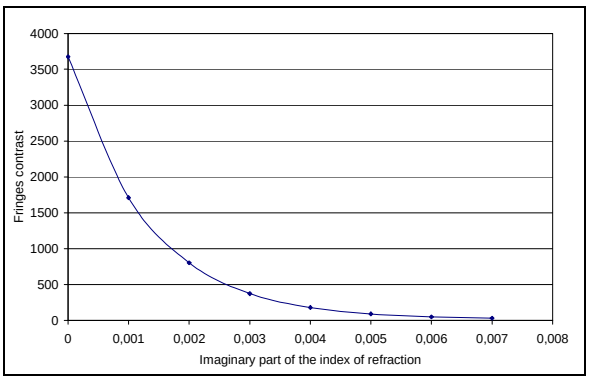

Figure 20. Relationship between the imaginary part of the optical index and the contrast of the fringes

We first notice that the frequency of the fringes is not modified by changes in the imaginary part of the optical index. Thus, the droplets size measurement can still be determined using exactly the same method as presented previously. Figure 20 presents the relationship between the imaginary part of the optical index and the contrast of the fringes.

With this optical configuration, we observe a biunivocal relationship between the contrast of the fringes and the imaginary part of the optical index. Thus, it would allow giving quantitative information of the number of aerosol particles collected by the droplets.

The limitations in this technique lie in the limit of solubility of aerosol particles inside the droplets. For example, if we consider potassium permanganate aerosols (for its absorbance spectrum, which maximum corresponds to our laser wavelength, Figure 21), its limit of solubility is S = 63.8 $g.L^{-1}$ in water.

Thus we determine the relations between the absorbance (A) and the optical index imaginary part (k) as a function of the light wavelength (λ), the potassium permanganate concentration ($[KMnO_4]$) and its molecular extinction cross section ε. The absorbance has been determined using a spectrometer which tank length is L.

$$n = m + ik \qquad (3)$$

$$A = \varepsilon_{KMnO_4} L[KMnO_4] = \frac{4\pi kL}{\lambda} = -\log\left(\frac{I_0}{I}\right) \qquad (4)$$

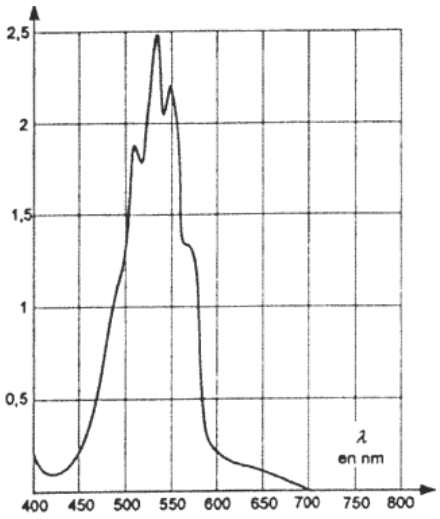

Figure 21. Absorbance spectra of potassium permanganate

Thus, using this technique the greater imaginary part of index of refraction measurable is limited by the crystal solubility.

$$k_{\max} = \frac{\varepsilon_{KMnO_4} S_{KMnO_4} \lambda}{4 M_{KMnO_4} \pi} \quad (5)$$

In this equation, the molecular extinction coefficient is determined using the absorption cross section of the potassium permanganate molecule $\left(\sigma_{KMnO_4}\right)$.

$$\varepsilon = \frac{1}{\ln 10} Na \sigma_{KMnO_4} \quad (6)$$

$$k_{\max} = \frac{Na\, \sigma_{KMnO_4} S_{KMnO_4} \lambda}{4 M_{KMnO_4} \pi \ln 10} = 3.64 \times 10^{-6} \quad (7)$$

As a consequence, we deduce that the visibilities of the fringes don't decrease enough with potassium permanganate concentration to allow to deduce precisely the concentration inside the droplet. This is mostly due to the low optical thickness of a droplet (approximately 100 µm).
Another way to measure the concentration of soluble aerosol is still to use soluble aerosol particles (there is no more need to be absorbent in the laser wavelength), and to determine the real part of the droplets index of refraction variation induced by crystal dissolution inside the droplet. For example, the relation between potassium chloride concentration and the associate variations of the index of refraction is plotted on Figure 22.

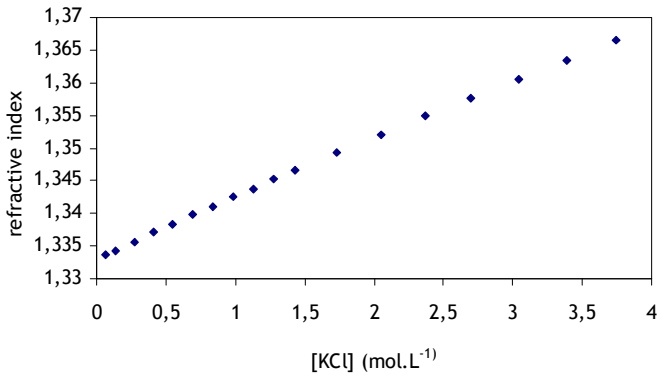

Figure 22. Influence of KCl concentration on water index of refraction

The Global Rainbow Refractometry is an efficient technique to measure droplets index of refraction [9]. It has been first developed on the TOSQAN experiment in order to measure droplets temperature, due to the fact that water index of refraction is sensitive to its temperature [6].
The rainbow is a phenomenon that occurs when a single droplet intercepts a laser beam (Figure 23). The interferences between internally reflected rays will induce a low frequency structure called Airy fringes. The interferences between internally and externally reflected rays will cause a high frequency structure called ripple structure superimposed on the Airy fringes (Figure 24). Using the Lorenz Mie theory, which consists in resolving the Maxwell's equations, we can compute the rainbow scattered by a single droplet. The standard rainbow refractometry is a non-intrusive technique for measuring size and temperature of a single spherical droplet.

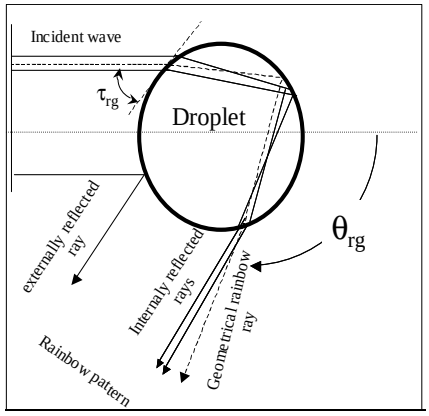

Figure 23. Rainbow phenomenon

In Figure 23, the "rg" index corresponds to the ray of geometrical rainbow. This ray is the one that has the minimum of deflexion after emerging the droplet. The scattering angle corresponding to this ray (θ_{rg}) only depends on the index of refraction (m) of the droplet, thus its detection allows us to determine droplets temperature. This technique, based on the analysis of the rainbow, suffers of major problems related to temperature gradients inside the droplet and droplet non-sphericity. For small particles, the ripple structure (issued from the interference between internally and externally reflected rays, Figure 23) strongly disturbs the rainbow pattern.

To overcome the last two problems, van Beeck introduced the global rainbow refractometry. The principle of the technique is to superimpose the rainbows patterns issued from enough droplets to be statistically representative of the spray, so that the ripple structure totally disappears. This phenomenon was first observed by Roth [9] for a single droplet with diameter variations ; the non-spherical droplets (as far as they are randomly oriented) will interfere destructively and will then create a uniform background, and consequently they will not disturb the measurement anymore.

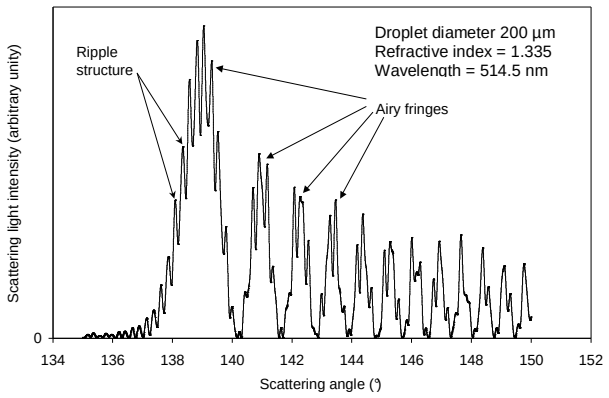

Figure 24.Standard rainbow pattern

It has been shown that this technique can measure index of refraction variations as low as one thousandth [6], which corresponds to a potassium chloride concentration variation of 0.1 mol.L^{-1}. As a consequence, the global rainbow refractometry in also a very efficient technique to characterise aerosol collection by droplets.

5 CONCLUSION

In this paper, we presented the implementation of the ILIDS technique on the TOSQAN experiment which is a large experimental vessel. The validation of the method was also performed using comparisons with PDA and backscattering measurements. Then, measurements were presented inside the TOSQAN experiment during a spray test.

Finally an extension of the method was proposed, in order to be able to measure the imaginary part of the optical index, and thus to characterize aerosol collection processes by droplets. Our computations highlight the difficulty to measure concentrations in droplets using the technique, due to the limit of solubility of the aerosols. Another technique, called Global Rainbow Refractometry, was proposed to determine, as an example, the real part of the index of refraction induced by the dissolution of a potassium chloride aerosols collected by the droplets. Our computations associated with previous measurement [6] achieved on droplets with temperature variations, highlight the efficency of this technique to determine potassium chloride concentration inside the droplet with a precision of 0.1 mol.L^{-1}.

REFERENCES

1. Bachalo, W.D., Houser, M.J., Phase/Doppler spray analyzer for simultaneous measurements of drop size and velocity distribution, Optical Engeenering, Vol. 23, No. 5, pp 583-590, 1984.
2. Glover, A.R., Skippon, S.M. and Boyle, R.D., Interferometric laser imaging for droplet sizing : a method for droplet-size measurement in sparse spray systems, Applied Optics, Vol. 34, No. 36, 1995.
3. Malet, J., Lemaitre, P., Porcheron, E., Vendel, J., Blumenfeld, L., Dabbene, F. and Tkatschenko, I., Benchmarking of CFD and LP codes for spray systems in Containment applications : spray tests at two different scales in the TOSQAN and MISTRA facilities, CFD4NRS, 2006.
4. Marchand, D., Porcheron, E., Lemaitre, P. and Grehan, G., Characterization of the washout of aerosols by spraying water for thermal hydraulics conditions representative of a severe accident in a nuclear reactor containment, 10th International Congress on Liquid Atomization and Spray Systems, Kyoto, Japan, August 27 - September 1, 2006.
5. Méès, L and Gréhan, G., Réfractométrie d'arc-en-ciel et imagerie en défaut de mise au point, Rapport LESP 06-03, Contrat IRSN-CORIA, DA 23275/CA 31000203, 2003.
6. Lemaitre, P., Porcheron, E., Grehan G. and Bouilloux L., Development of the global Rainbow refractometry to measure spray droplets temperature in a large containment vessel, Measurement Science and Technology, 2006.
7. Porcheron, E., Thause, L., Malet, J., Cornet, P., Brun, P. and Vendel, J., Simultaneous application of Spontaneous Raman Scattering and LDV / PIV for steam / air flow characterization, 10th International Symposium on Flow Visualization, Kyoto, Japan, 26-29 august, 2002.
8. Porcheron, E., Lemaitre, P., Nuboer, A., Vendel J. and Bouilloux L., Experimental investigation of heat and mass transfers in a spray inside the TOSQAN facility for nuclear reactor containment safety, 10th International Congress on Liquid Atomization and Spray Systems, Kyoto, Japan, August 27 - September 1, 2006
9. Roth N. , Andens K., Frohn A., Refractive-Index Measurement for the Correction of Particle sizing methods. Applied optics 30 pp : 4946-4965, 1991.
10. van de Hulst, H.C., Light scattering by small particles, Dover Publications, pp.13-249, 1981.
11. Thormählen, J., Straub, U. and Grigull, Refractive index of water and its dependence on wavelength temperature and density, Journal of Physical Chemistry, Ref. data 14, 1985.